doi:10.1093/brain/awx369 BRAIN 2018: 141; 662–672 | 662

BRAIN
A JOURNAL OF NEUROLOGY

SCO2 mutations cause early-onset axonal Charcot-Marie-Tooth disease associated with cellular copper deficiency

Adriana P. Rebelo,[1] Dimah Saade,[2] Claudia V. Pereira,[3] Amjad Farooq,[4] Tyler C. Huff,[3] Lisa Abreu,[1] Carlos T. Moraes,[3] Diana Mnatsakanova,[2] Kathy Mathews,[2] Hua Yang,[5] Eric A. Schon,[5,6] Stephan Zuchner[1,*] and Michael E. Shy[2,*]

*These authors contributed equally to this work.

Recessive mutations in the mitochondrial copper-binding protein SCO2, cytochrome *c* oxidase (COX) assembly protein, have been reported in several cases with fatal infantile cardioencephalomyopathy with COX deficiency. Significantly expanding the known phenotypic spectrum, we identified compound heterozygous variants in *SCO2* in two unrelated patients with axonal polyneuropathy, also known as Charcot-Marie-Tooth disease type 4. Different from previously described cases, our patients developed predominantly motor neuropathy, they survived infancy, and they have not yet developed the cardiomyopathy that causes death in early infancy in reported patients. Both of our patients harbour missense mutations near the conserved copper-binding motif (CXXXC), including the common pathogenic variant E140K and a novel change D135G. In addition, each patient carries a second mutation located at the same loop region, resulting in compound heterozygote changes E140K/P169T and D135G/R171Q. Patient fibroblasts showed reduced levels of SCO2, decreased copper levels and COX deficiency. Given that another Charcot-Marie-Tooth disease gene, *ATP7A*, is a known copper transporter, our findings further underline the relevance of copper metabolism in Charcot-Marie-Tooth disease.

1 Dr. John T. Macdonald Foundation Department of Human Genetics and John P. Hussman Institute for Human Genomics, University of Miami Miller School of Medicine, Miami, USA
2 Department of Neurology, Carver College of Medicine, University of Iowa, Iowa City, USA
3 Department of Neurology, University of Miami, Miami, USA
4 Biochemistry Department, University of Miami Miller School of Medicine, Miami, USA
5 Department of Neurology, Columbia University Medical Center, New York, USA
6 Department of Genetics and Development, Columbia University Medical Center, New York, USA

Correspondence to: Dr Michael E. Shy
Department of Neurology
Carver College of Medicine
2007 Roy Carver Pavilion, 200 Hawkins Drive
Iowa City, IA 52242, USA
E-mail: michael-shy@uiowa.edu or m.shy@wayne.edu

Keywords: Charcot-Marie-Tooth disease; SCO2; copper deficiency

Abbreviations: CMT = Charcot-Marie-Tooth; COX = cytochrome *c* oxidase

Received June 19, 2017. Revised November 7, 2017. Accepted November 14, 2017. Advance Access publication January 16, 2018

Introduction

SCO2 [cytochrome *c* oxidase (COX) assembly protein] is a mitochondrial copper binding protein important for the assembly of COX, complex IV of the mitochondrial respiratory chain (Horng *et al.*, 2005). Several assembly factors are required for the assembly of COX; four of those assembly genes, *SCO1*, *SCO2*, *COX10* and *SURF1* have been identified in mitochondrial disorders associated with a wide range of clinical phenotypes (Barrientos *et al.*, 2002). SCO2 and its homologue SCO1 are metallochaperones that play an essential role in the biogenesis and maturation of the catalytic COXII subunit (Williams *et al.*, 2005; Soto *et al.*, 2012). SCO1 and SCO2 contain a highly conserved copper-binding motif (CXXXC) important for the insertion of copper into COXII (Banci *et al.*, 2007). Autosomal recessive mutations in both *SCO1* and *SCO2* cause severe early onset mitochondrial disorders associated with complex IV deficiency (Papadopoulou *et al.*, 1999). Although SCOs have similar functions, they cause distinct clinical phenotypes. Recessive mutations in *SCO1* can cause severe neonatal hepatopathy, encephalopathy or hypertrophic cardiomyopathy (Valnot *et al.*, 2000; Leary *et al.*, 2013) (MIM: 220110). Recessive mutations in SCO2 have been predominantly associated with fatal infantile cardioencephalomyopathy (MIM: 604377) characterized by severe COX deficiency (Papadopoulou *et al.*, 1999). In addition, SCO1 and SCO2 may also play a role in cellular copper homeostasis (Leary *et al.*, 2007) as mutations have been shown to result in severe copper deficiency in affected tissues (Leary *et al.*, 2007). Copper dysregulation has been recognized as a pathological feature of neurodegenerative diseases including: Alzheimer's, Parkinson's, Menkes and Wilson diseases. Mutations in the copper transporters ATP7A and ATP7B cause Menkes and Wilson diseases, respectively (Telianidis *et al.*, 2013). Interestingly, causative ATP7A mutations have also been described in patients with distal hereditary motor neuropathy (dHMN) (Kennerson *et al.*, 2010).

Here, we describe a motor-predominant peripheral neuropathy phenotype in two unrelated patients with compound heterozygous mutations in *SCO2*. Remarkably, the *SCO2* mutations in our patients have not resulted in cardioencephalomyopathy or a fatal outcome as is typical for SCO2 disease. Analysis of patient fibroblast lines revealed decreased SCO2 protein amounts, COXII deficiency and reduced copper levels. These findings expand the phenotypic spectrum of SCO2 mutations and further support copper deficiency as a mechanism in peripheral neuropathies.

Materials and methods

Patient recruitment

We recruited patients from the University of Iowa CMT Clinic. All study participants consented under an IRB approved research protocol. The data used include EMG test results, neurology evaluation/consultation, and genetic testing for Charcot-Marie-Tooth (CMT) or exome sequencing.

Whole-exome and Sanger sequencing

Whole-exome sequencing was performed in the two index individuals with autosomal-recessive CMT4. The SureSelect Human All Exon Kit (Agilent) was used for in-solution enrichment, and the HiSeq 2500 instrument (Illumina) was used to produce 100 bp paired-end sequence reads. The Burrows-Wheeler aligner and Freebayes were used for sequence alignment and variant calling. Exome data were uploaded into the GENESIS software and analysed. Sanger sequencing confirmed the *SCO2* missense variants detected by whole-exome sequencing.

Structural modelling

Structural model of the wild-type and mutant C-terminal ordered region of human SCO2 (residues 101–266) were built using the MODELLER software based on homology modelling (Marti-Renom *et al.*, 2000). Briefly, the crystal structure of the homologous human SCO1 in complex with a Cu^{+} ion (PDBID 2GQM) was used as a template in each case. It should be noted that over 50% of residues within the C-terminal ordered regions of human SCO1 and SCO2 are identical, as determined by pairwise sequence alignment using Clustal Omega (Sievers *et al.*, 2011). With such high level of sequence identity between the template and model, the structural model presented here can be relied upon with a very high degree of confidence. A total of 100 atomic models were calculated and the structure with the lowest energy, as judged by the MODELLER Objective Function, was selected for further analysis in each case. The structural models were rendered using RIBBONS (Carson, 1991).

Cell culture

Fibroblasts cells were obtained from affected patients and control patient by skin biopsies and grown in Dulbecco's modified Eagle medium containing 10% (v/v) foetal bovine serum under humidified air at 37°C in 5% CO_2.

Analysis of copper in fibroblast using induced coupled-mass spectrometry (ICP-MS)

Fifty milligrams of fibroblasts were collected and submitted for induced coupled-mass spectrometry (ICP-MS) analysis at Nano Research Facility (Washington University in St. Louis). Digestion procedure: 1 ml of concentrated nitric acid was added to each sample and placed in Mars 6 Microwave Digestion System (CEM coporation) set to 200°C for 20 min.

Western blot

The following antibodies were used for western blot analysis: rabbit anti-SCO2 (Abcam), rabbit anti-TOM20 (Santa Cruz),

mouse anti-MTCO2 (Abcam) and mouse anti-actin (Sigam-Aldrich).

Semithin sectioning

Sciatic nerves were dissected from 8-month-old homozygous knock-in and 4-month-old *Sco2* compound heterozygous and wild-type c57bl/6j mice. Nerves were fixed in 3% glutaraldehyde 4% paraformaldehyde in 0.1 M phosphate buffer overnight at 4°C and subsequently placed in 30% sucrose until processed. Nerves were post-fixed with 2% osmium tetroxide and subsequently dehydrated using a graded ethanol series (50%, 75%, 95%, 100%). After dehydration, nerves were embedded in Spurr's resin (EMS, Cat# 14300), polymerized at 80°C overnight, and sectioned at 1 µm for light microscopy using an EM UC6 ultramicrotome (Leica). Semithin sections (1 µm) were transferred to glass slides, stained with 1% alkaline toluidine blue solution and photographed with the Nikon Eclipse TE2000-U. G-ratio, axon diameter, and fibre diameter measurements were executed using FIJI (ImageJ).

Complex IV and citrate synthase activities

Cell pellets containing ~1 million cells were collected and resuspended in 100 µl of 50 mM KH_2O_4, pH 7.2, 1.5% dodecyl maltoside plus protease inhibitors (cOmplete™ Mini Protease Inhibitor Cocktail, Roche). The samples were kept on ice for 30 min before centrifugation at 14 000*g* for 15 min, at 4°C. The supernatants were transferred to new centrifuge tubes and the protein concentration was determined with the DC protein assay (5000116, Bio-Rad), according to the manufacturer's instructions. Complex IV activity was determined spectrophotometrically in 96-well format in a BioTek Synergy H1 hybrid plate reader at 550 nm in kinetic mode, at 37°C. The reaction started with the addition of the sample to 200 µl of reaction solution containing 20 mM KH_2PO_4 pH 7.2, 0.015% dodecyl maltoside (D4641, Sigma-Aldrich) and 40 µM of reduced cytochrome *c* (C2506, Sigma-Aldrich). Complex IV activity was calculated in the linear range and KCN (60178-25g, Sigma-Aldrich) was added in some wells, to ensure specificity. The assay results were normalized to the average of protein concentration measured before and after the assay. Citrate synthase activity was determined with the same cell samples spectrophotometrically in 96-well format at 412 nm in kinetic mode at 30°C. The reaction in the absence of the substrate oxaloacetate (O-4126 Sigma-Aldrich) was first determined for 1 min by adding the sample to 200 µl of reaction solution containing 10 mM Tris-HCl pH 7.5, 200 µM acetyl-CoA, 100 µM of DTNB and 0.2% Triton™ X-100. Then, 0.5 mM of oxaloacetate was added and the rate was measured for ~15 min. Citrate synthase activity was calculated in the linear phase and normalized to protein amount. The data were also analysed by calculating the ratio of complex IV and citrate synthase activities.

Oxygen consumption rate

Cells were grown for 1 week in low glucose (1 g/l) media (10567014, Thermo Scientific) and seeded at a density of 20 000 cells/well/100 µl in a XFp microplate. Oxygen consumption was measured at 37°C using a Seahorse XFp Extracellular Flux Analyzer (Seahorse Bioscience). Measurements of endogenous respiration were performed with Seahorse media supplemented with 1 mM pyruvate, 2 mM glutamine and 10 mM glucose. The oxygen consumption rates were analysed by the sequential injection of 1 µM of oligomycin, 2 µM of FCCP and 1 µM of rotenone plus antimycin A. All oxygen consumption rates and bioenergetic parameters were determined as indicated in the Excel report generator from Wave Software. The results were normalized to micrograms of protein quantified after each Seahorse run, with the DC protein assay, as described above.

Results

Clinical description of patients with CMT4

Patient 1

Patient 1 presented with subtle early gross motor delay, she was unable to lift her head up from prone position at 6 months and she toe walked at 15 months. As a toddler she did not keep up with her peers, was clumsy with frequent falls and required ankle foot orthotics at 3 years of age. She never ran or jumped. She had recurrent exotropia and underwent surgery twice.

Initial work up at 2 years of age included a normal brain MRI and creatinine kinase. Thigh muscle biopsy revealed chronic denervation atrophy raising the concern for spinal muscular atrophy (SMA). Succinate dehydrogenase and COX histochemical reactions were normal. *SMN1* deletion and sequencing assays were normal. EMG/nerve conduction studies revealed length dependent, motor predominant axonal polyneuropathy. She was therefore diagnosed with infantile onset axonal CMT. Commercial gene CMT (through Athena) was non-revealing.

She first presented to our clinic at 5 years of age. At the time she was ambulating with full time use of ankle foot orthotics. Her exam revealed exotropia and bilateral ptosis in addition to significant distal upper and lower extremity muscle wasting. She was able to plantar flex her feet but had no distal lower extremity movements otherwise. Reflexes were absent and she walked with difficulty with a steppage gait. Her initial recent CMT neuropathy score (CMTNS)-2 score was 21/36, indicating severe impairment. Research-based trio whole exome sequencing revealed two parentally inherited mutations in *SCO2*; E140K, a rare mutation associated with mitochondrial disease; and P169T, a private mutation predicted to be pathogenic.

When she returned to our clinic at 9 years of age she had been using a power wheelchair full time for over 4 years. She could bring her hands up to her face if her elbows were propped up and needed assistance cutting and eating her food and writing. Her cranial nerve exam revealed bilateral ptosis, facial weakness with a flat smile, facial fasciculation and dysarthria. Motor exam was remarkable for proximal

and distal weakness in arms and legs and absent reflexes. Sensory exam was normal except for mildly diminished vibratory sense at the toes. Her most recent CMT Examination Score (CMTES)-2 was 17/28 (CMTES-2 differs from CMTNS-2 in that nerve conduction studies were not repeated). Serum lactate was mildly elevated but lactate to pyruvate ratio was normal. Serum copper and ceruloplasmin, ECG and echocardiogram were within normal.

Both parents are clinically unremarkable. EMG studies of both parents were normal, including normal conduction velocities and normal compound muscle action potentials. However, interestingly, both parents of Patient 1 have *pes cavus* indicating a potential subclinical peripheral neuropathy. We interpret this as subclinical carrier status.

Patient 2

Patient 2 presented at 12 years of age with inability to keep up with peers, heel cord tightness and progressive foot drop. His initial exam at 22 years revealed wasting of distal lower extremities and flat feet. He had weakness of tibialis anterior and gastrocnemius muscles (MRC grading 2/5), steppage gait and abolished ankle deep tendon reflexes. He had no sensory complaints but exam revealed decreased vibratory sensation in toes and ankles. EMG and nerve conduction studies showed a length dependent axonal sensorimotor polyneuropathy. His initial CMTNS-2 score was 8/36 indicating mild impairment.

He was diagnosed with childhood onset axonal CMT. *MFN2* sequencing was normal. Research-based trio whole exome sequencing revealed two parentally inherited mutations in *SCO2*; R171Q (rare, R171W is associated with mitochondrial disease); and N135F (private), predicted to be pathogenic and determined to be causative. At his most recent evaluation at 26 years of age he remained ambulatory with full time use of ankle foot orthotics. He is gainfully employed as a mechanic. He now has mild difficulty fastening buttons and hand cramping with repetitive tasks such as screwing in plug drains. Exam revealed striking lower leg atrophy, pes planus and progressive distal lower extremity weakness with inability to dorsi flex, plantar flex, evert or invert feet. Reflexes were present and normal at the biceps, triceps and knees but absent at the ankles. Vibratory sensation was diminished at the toes and ankles. His most recent CMTES-2 score remained in the mild impairment range, 7/28.

Serum copper, ceruloplasmin, lactate and pyruvate were all within normal limits. Electrocardiogram showed premature ventricular contractures (PVCs) but was otherwise unremarkable. Due to complaint of chest pain and palpitations a 24-h Holter monitoring was obtained and revealed an increased PVC frequency (30%). Echocardiogram was normal. Exercise stress ECG was normal with decrease in PVC frequency with exercise. He was referred to cardiac electrophysiology for consideration of medication therapy versus cardiac electrophysiological study and potential ablation. Table 1 summarizes patient's characteristic features.

Identification of *SCO2* variants in patients with CMT4

We performed whole-exome sequencing in two unrelated index patients of European ancestry diagnosed with axonal CMT. Exome data were analysed with a strict filtering approach for conservation, function and allele frequency using the GENESIS software (Gonzalez *et al.*, 2013). Because both cases were sporadic, we analysed heterozygous, homozygous and compound heterozygous variants. Mutations in known CMT genes were absent in both families. *SCO2* was identified as the top candidate gene with compound heterozygous variants in both patients (Supplementary Table 1). All *SCO2* variants identified were predicted to be functionally damaging and positioned at highly conserved regions. Index Patient 1 carries the previously identified 'common' pathogenic variant c.418G>A (p.E140K) at chr22:50,962,423 and a 'private' variant c.505C>A (p.P169T) at chr22:50,962,336. The latter change has not been reported in large public databases (Exome Variant Server, ExAc, 1000 genomes, dbSNP). Index Patient 2 carries a private variant located at the copper-binding site c.404A>G (p.D135G) at chr22:50,962,437 and another rare variant, c.512G>A (p.R171Q) at chr22:50,962,329, located at the same position of a previously reported pathogenic variant R171W. Sanger sequencing was performed to confirm a compound recessive trait and co-segregation of these alleles with the phenotype (Fig. 1A). The compound heterozygous variants in the studied CMT families are located close to each other in the conserved thioredoxin domain (Fig. 1B). Family 1 variant E140K is adjacent to the copper-binding site, similarly Family 2 variant D135G is located within the highly conserved copper-binding motif CXXXC (Fig. 1B). The other two variants P169T and R171Q, from Families 1 and 2, respectively, are located at the same loop region close to the copper-binding site (Fig. 2).

Structural modelling predicts disruption in the copper-binding site by *SCO2* mutations

To understand the molecular basis of how the mutations identified here (D135G, E140K, P169T, and R171Q) may affect the physiological function of SCO2, we modelled the wild-type and mutant structures of its C-terminal ordered region (residues 101–266) bound to a Cu^+ ion. As shown in Fig. 2, SCO2 adopts a thioredoxin fold with a central highly-curved seven-stranded antiparallel β-sheet sandwiched between three α-helices on one side and one α-helix on the other. Importantly, this latter α-helix feeds into a β-hairpin that serves as an extended lid over the copper-binding site within which the Cu^+ ion is coordinated by two highly conserved cysteine residues (C133/C137), located within the CXXXC motif, and an histidine residue (H224). Strikingly, the copper-binding site is

Table 1 Clinical characteristics of patients

ID	Mutations	Age at onset	Age at most recent exam, y	Presenting symptom	Motor exam Strength MRC scale 0–5[a]	Sensory exam	Additional findings	CMTNS-2 score[b]	Laboratory tests	Cardiac	EMG/NCS
1	E140K, P169T	Infancy	9	Toe walked at 15 months	Deltoids 2, biceps 3, triceps 4, wrist extensors/flexors 2, FDI/APB 2, ADM 0, iliopsoas 4, quadriceps 2, hamstrings 4, TA, gastrocnemius, foot eversion/inversion, great toe plantar/dorsiflexion 0	Decreased vibration at toes	Ptosis, facial weakness, facial fasciculation, dysarthria	17/28	Lactate 3.5 mmol/l (0.7–2.1), pyruvate 0.174 mmol/l, ratio: 20:1 Cu 128 μg/dl (70–140) ceruloplasmin 26 mg/ml (16–66)	Normal ECG and echo	Ulnar CMAP: 0.3 mV Ulnar motor CV: 44 m/s
2	R171Q, N135F	12	26	Foot drop, inability to keep up with peers	TA, gastrocnemius, foot eversion/inversion, great toe plantar/dorsiflexion 0 Otherwise normal strength	Decreased vibration at toes		7/28	Lactate 1.47 mmol/l, pyruvate 0.071 mmol/l, ratio:19.7 Cu 92 μg/dl, ceruloplasmin 23 mg/dl	Frequent PVCs on 24-h holter monitoring (30%) Normal echocardiogram and stress ECG Referred to electrophysiology	Tibial motor response absent, peroneal motor response recorded from TA 0.32 mV, CV 43 m/s (across the knee) Radial and sural sensory responses absent. Ulnar SNAP 0.002 mV, CV 54 m/s. High amplitude, reduced recruitment and polyphasic motor unit potentials in TA and FDI

[a]MRC medical research council scale for muscle strength.

[b]CMT Neuropathy Score (CMTNS) version 2 (CMTNSv2) score was calculated using a modified CMTNS that had been validated previously as a measure of disability due to CMT.

ADM = abductor digiti minimi; APB = abductor pollicis brevis; CMAP = compound muscle action potential; CV = conduction velocity; FDI = first dorsal interosseous; NCS = nerve conduction study; PVC = premature ventricular contractures; TA = tibialis anterior.

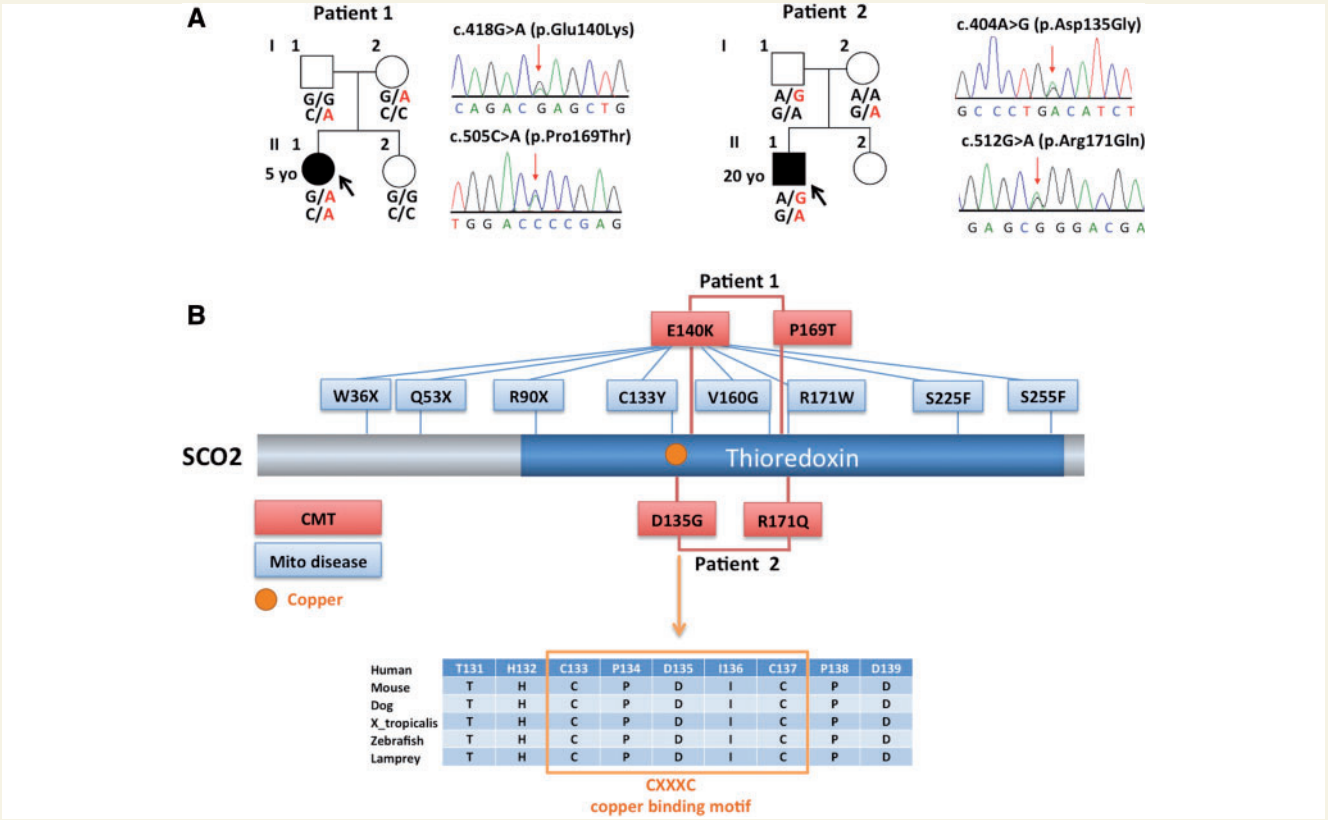

Figure 1 SCO2 mutations in autosomal recessive CMT families. (**A**) Pedigree and Sanger Sequence traces of CMT4 families with compound heterozygous mutations in SCO2. (**B**) Diagram shows variants in red associated with CMT and variants in blue associated with the mitochondrial disease fatal infantile cardioencephalopmyopathy. Protein alignment across different species shows conservation of copper-binding motif.

flanked by amino acids such as D135, E140, P169, and R171 (Fig. 2A and B). Not only such residues appear to be critical for the optimal configuration and organization of a native copper-binding site but they may also aid the entry of Cu^+ ion into SCO2 from the surrounding milieu and/or its delivery to Complex IV. More specifically, D135 and E140 respectively form ion pairs with neighbouring R243 and K143 on one side of the copper-binding site. On the other side, P169 appears to induce a sharp kink within a loop region so as to mediate the formation of an additional ion pair between R171 and D168 close to the copper-binding site. Such ion pairs most likely serve as ties or stitches that ensure the integrity of the copper-binding site. Accordingly, disruption of one or more aforementioned ion pairs would be fraught with serious structural damage resulting in protein dysfunction (Fig. 2C and D).

Taken together, our structural analysis strongly suggests that mutations such as D135G, E140K, P169T, and R171Q would likely result in the structural distortion of the copper-binding site within SCO2. The failure of SCO2 to bind and deliver copper to complex IV within the mitochondrial respiratory chain would hamper the ability of rapidly respiring cells to meet their energy needs. Our structural analysis thus provides a rationale at molecular level for the role of SCO2 in the onset and development of neuromuscular disorders such as CMT.

Patients' fibroblasts have decreased levels of SCO2, COXII and copper levels

To investigate the impact of *SCO2* mutations at the molecular level, patients' fibroblasts were collected for analysis. Because the steady-state levels of mutant SCO2 in patients with fatal infantile cardioencephalomyopathy are severely reduced in patient tissues (heart, brain, liver and fibroblasts) (Stiburek *et al.*, 2005), we evaluated SCO2 levels in our patient's fibroblasts. Western blots probed with a SCO2 antibody show significant reduction in SCO2 protein levels in both patients (Fig. 3A). SCO2 levels were more significantly reduced in Patient 1, who is also more severely affected than Patient 2, suggesting that SCO2 levels might reflect the severity of the disease. Mitochondrial protein levels measured by TOM20 were normal, indicating that mitochondrial biogenesis was not affected by the reduced levels of SCO2. However, the levels of COXII were also significantly reduced, indicating a direct effect of SCO2 on COXII stability (Fig. 3A). Next, we performed ICP-MS to measure the total copper levels in patient's cells. Copper levels were reduced three-fold in both patient's fibroblasts compared to control ($P < 0.0001$) (Fig. 3B). These results suggest that both mitochondrial dysfunction and copper dysregulation

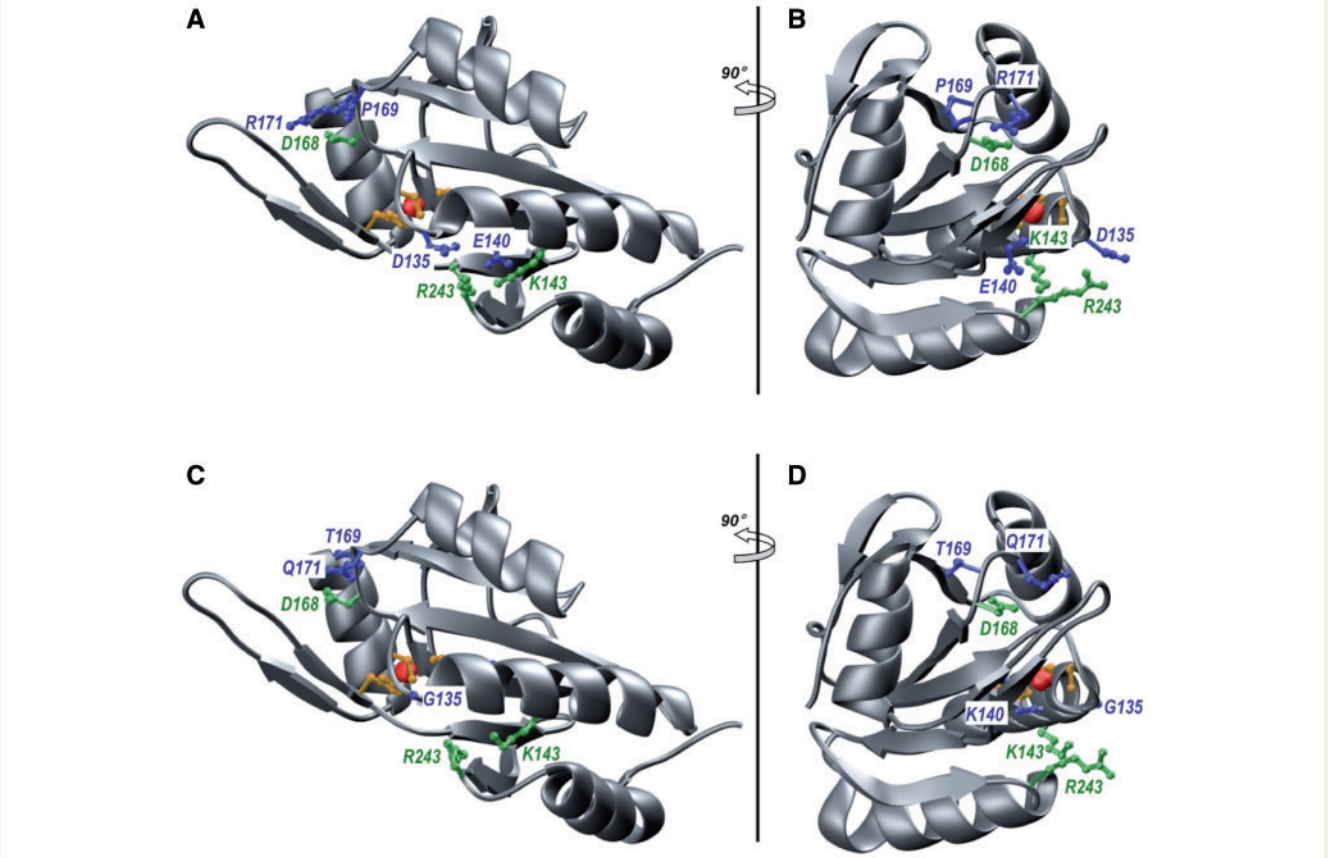

Figure 2 Ribbon representation of the structural model of wild-type (A and B) and mutant (C and D) C-terminal ordered region of human SCO2 (residues 101–266). The mutant model harbours D135G, E140K, P169T, and R171Q substitutions. Two orientations, related by a 90° rotation about the vertical axis, are provided in each case. The protein backbone is coloured grey. The sidechain moieties of D135/E140/P169/R171 residues (**A** and **B**) and their mutant counterparts (**C** and **D**) are coloured blue. The sidechain moieties of K143/D168/R243 residues that form ion pairs with E140/R171/D135 are coloured green. The sidechain moieties of the C133/C137/H224 triad that coordinates the Cu^{+} ion (depicted as a red sphere) are coloured yellow.

might be the pathological mechanism of the disease in those patients.

Mitochondrial function evaluation of patient's fibroblasts

COX is the terminal electron acceptor of the mitochondrial electron transport chain, which catalyses the transfer of electrons from reduced cytochrome *c* to molecular oxygen to form water and generates an electrochemical gradient that drives ATP synthesis. Therefore, to determine whether the cultured fibroblasts from patients with SCO2 mutations reveal complex IV activity dysfunction we have measured complex IV and citrate synthase activities (Fig. 4A–C). Surprisingly, Patient 1 did not show decreased complex IV activity when normalized by total protein (Fig. 4A) but when analysing citrate synthase activity there was a significant increase when compared to the control (Fig. 4B). Thus, the ratio of complex IV/citrate synthase activities was significantly decreased when compared to the control (Fig. 4C). In contrast, Patient 2 showed a significant decrease in complex IV activity, when normalized to either total protein or citrate synthase activity (Fig. 4A–C), in spite of the milder phenotype associated with this patient.

It is relatively common to find a lack of phenotype in human fibroblasts carrying mutations despite biopsies from tissues showing the contrary. To better mimic the physiological cellular growth conditions and to prevent possible metabolic adaptations in high glucose concentrations, the cell media was replaced with low glucose for 2 weeks. The cells did not show any growth arrest when compared to high glucose conditions, as the cell number yield was the same under both tested conditions. To further evaluate mitochondrial function, the oxygen consumption rate was determined with Seahorse XFp. Our results showed no significant differences between control and patient cells for all the tested bioenergetic parameters, although experimental variability was observed (Fig. 4D and E).

Examination of sciatic nerve semithin section from E140K mouse models

We analysed the sciatic nerves from E140K homozygous knock-in mice and compound heterozygous mice generated

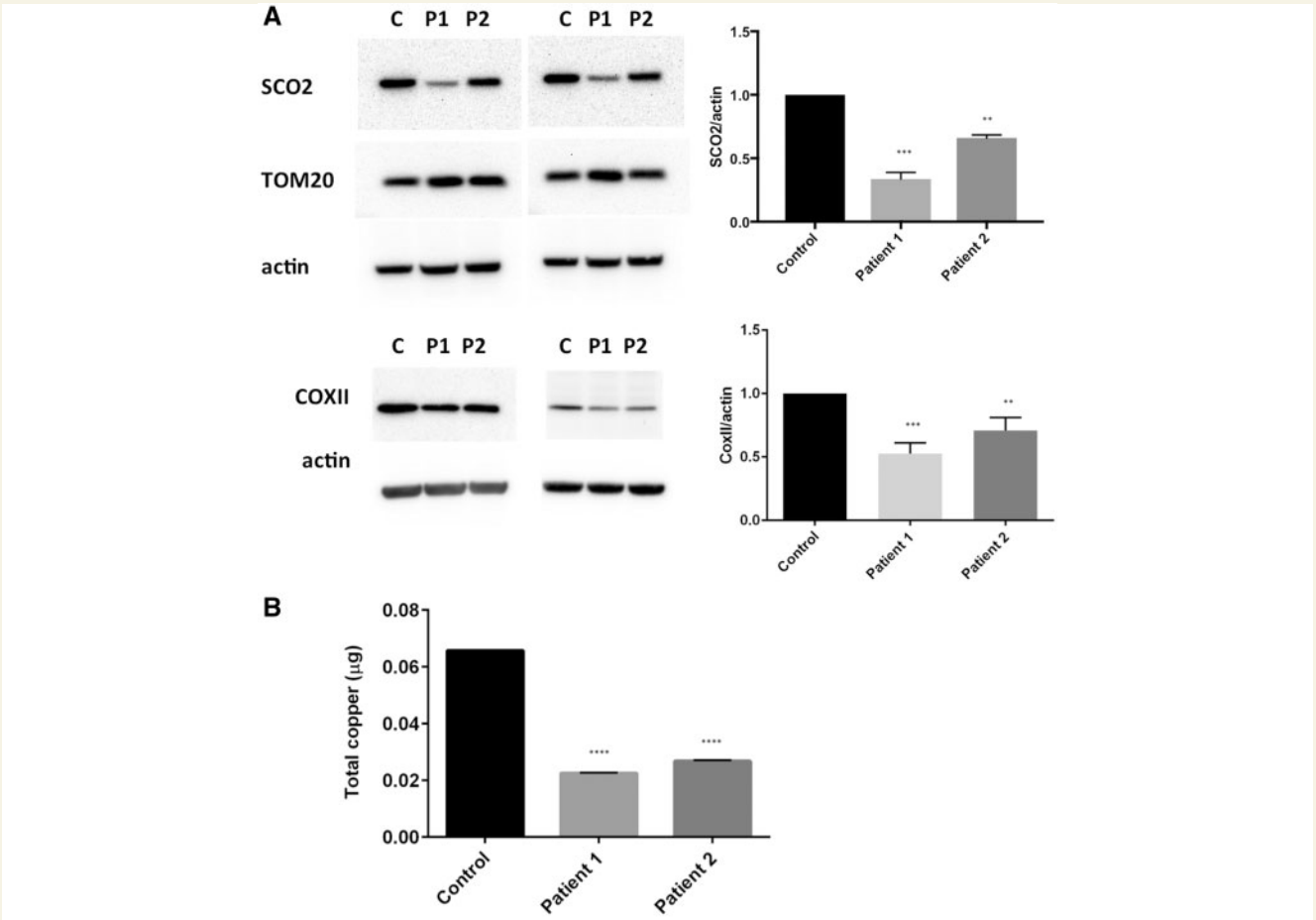

Figure 3 Fibroblasts from patients show decreased levels of SCO2, COXII and copper levels. (**A**) Western blot shows decreased levels of SCO2 and COXII in Patients 1 and 2. One-way ANOVA with Tukey's multiple comparisons test: control versus Patient 1 ($P < 0.001$), control versus Patient 2 ($P < 0.01$). (**B**) Copper levels measured by ICP-MS were significantly reduced in both patients. One-way ANOVA with Tukey's multiple comparisons test: control versus Patient 1 ($P < 0.0001$), control versus Patient 2 ($P < 0.0001$).

by Yang *et al.* (2010). Both mice were viable, but developed impaired motor functions assessed by behavioural tests. The compound heterozygote mice were more severely affected than the homozygous knock-in mice, and developed muscle weakness at 4 months of age (Yang *et al.*, 2010). Semithin sections of sciatic nerve from 10-month-old SCO2 homozygous knock-in and 4-month-old compound heterozygous mice showed no indication of nerve degeneration, such as, axonal loss or local axonal sprouting (data not shown). Although E140K mice show COX deficiency and muscle weakness, they do not recapitulate the neuropathy phenotype observed in our patients. One hypothesis for this discrepancy is that these mice might not live long enough to develop the neuropathy phenotype. Patients start developing a neuropathy phenotype later in childhood or early adolescence, but not during their first months of life. Alternatively, mice might have a greater redundancy in their copper metabolism. The lack of neuropathy-related phenotypes has been reported in other mouse models for neuropathy genes (Seburn *et al.*, 2014; Strickland *et al.*, 2014).

Discussion

SCO2 is a mitochondrial protein that serves as a copper chaperone that picks up a monovalent copper (Cu^+) ion and delivers it to the so-called CuA site within complex IV (COX)—the terminal enzyme within the respiratory chain involved in the reduction of molecular oxygen to water. SCO2 mutations are associated with fatal infantile cardioencephalomyopathy with COX deficiency (Papadopoulou *et al.*, 1999). The secondary phenotypic features associated with the lethal SCO2 mutations can be heterogeneous. Neurogenic features including spinal muscular atrophy has been previously reported along with hypertrophic cardiomyopathy, the main clinical feature in patients with SCO2 mutations (Supplementary Table 2). Interestingly, CMT Patient 1 also developed ptosis and strabismus, features that have also been reported in some patients with fatal infantile cardio encephalomyopathy (Pronicki *et al.*, 2010). Previous reports also described brain atrophy, seizures, gliosis and motor neuropathy revealed by nerve conduction studies (Papadopoulou *et al.*, 1999).

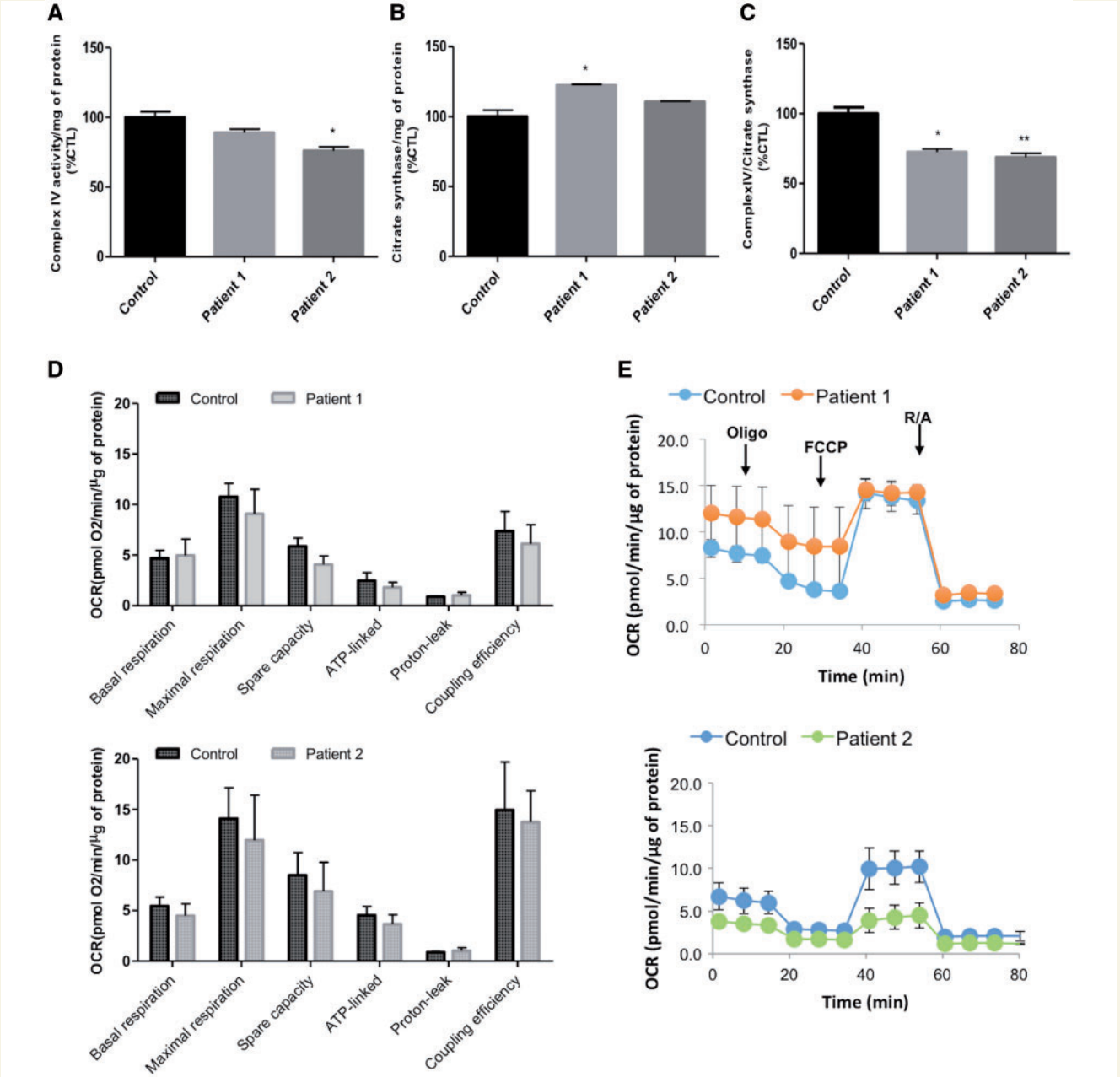

Figure 4 Patient fibroblasts show reduced complex IV/ citrate synthase activities but no significant differences in oxygen consumption rate. (**A**) Spectrophotometrically determined complex IV (CIV) activity is significantly decreased in Patient 2, when normalized to protein amount. Patient 2 complex IV activity was similar to the control. (**B**) Citrate synthase (CS) activity of Ptient 1 is significantly increased whereas there is no difference between the control and Patient 2. (**C**) Complex IV activity normalized to citrate synthase activity show that both Patients 1 and 2 have a significantly lower activity when compared to the control. Statistical analysis was performed with one-way ANOVA followed by the Bonferroni multiple comparison test. $*P < 0.05$, $**P < 0.01$, control versus patient. (**D**) Representative graph displaying the oxygen consumption rate (OCR) of control and patient cells (blue line, control; orange line, Patient 1 and green line, Patient 2). Oligomycin (Oligo), FCCP and rotenone plus antimycin A (R + A) were sequentially injected in each well. The error bars indicate the mean ± standard deviation of triplicates of one experiment. The bioenergetic parameters were not significantly different between the control and patients. Data analysis is presented as mean ± standard error of the mean of three separate experiments (duplicates or triplicates of each sample were analysed each time).

Although hypertrophic cardiomyopathy is the clinical hallmark and the main cause of foetal lethality in diseases associated with SCO2 mutations, our CMT patients have a distinct clinical phenotype. The reason for that variability in phenotype is not clear; however, there might be a correlation between location and combination of the variants with the clinical phenotype. We speculate that the specific mutations we observed and/or their combination results in

less damage to specific protein functions. The observed mutations do not seem to affect mitochondrial respiration, but still caused severe copper deficiency in fibroblasts (Fig. 3B). Another possibility is that genetic or environmental modifiers lead to the distinct phenotype observed in our patients. Because cardioencephalomyopathy patients die in early infancy due to heart failure, physicians may not evaluate peripheral neuropathy, which might be a minor or subclinical feature in those patients, as observed by Pronicki *et al.* (2010). Short lifespan could also explain the absence of a neuropathy in the *Sco2* compound heterozygous mice. Thus, screening patients with *SCO2* cardioencephalomyopathy for signs of neuropathy will be important to establish the clinical neuropathy component.

The most severely affected CMT patient carries the common pathogenic mutation, E140K in combination with a novel strong variant P169T. CMT Patient 2 has two novel strong variants, one missense mutation right at the copper-binding motif (CXXXC), D135G, in combination with the missense R171Q, at a previously reported pathogenic position with a different amino acid change (R171W). The E140K is the most common variant observed in the lethal disease, it is usually combined with a second variant in a compound heterozygous state. The E140K variant is also commonly seen in combination with non-sense variants resulting in truncated proteins, which would confer complete loss-of-function for one allele. Interestingly patients homozygous for E140K developed a later onset and milder clinical presentation, which suggests that E140K is the least damaging variant. The presence of the E140K variant in one of our patients with significantly milder phenotypes compared to lethal cases, confirms that mutation has only a partial loss-of-function. It has been suggested that E140K might affect the ability to bind copper and cause protein structural instability (Papadopoulou *et al.*, 1999; Leary *et al.*, 2004). Because copper is positively charged, a mutation that replaces a negatively charged into a positive charged amino acid (E to K) would destabilize copper binding (Papadopoulou *et al.*, 1999). Western blot analysis of our patient's fibroblasts show reduced levels of SCO2 suggesting protein instability. SCO2 stability seems to correlate with disease severity, since lethal cases have immunologically undetectable SCO2, in contrast to our least severely affected (Patient 2) who presented the highest SCO2 levels. COXII was also reduced as a result of decreased SCO2 leading to complex IV deficiency. In addition, CMT patient's fibroblasts show a significant reduction in total copper level. It is not clear how COX deficiency can lead to CMT and not a mitochondrial disease; however, this is not the only reported COX assembly gene associated with CMT. Mutations in *SURF1*, another COX assembly gene, also cause a recessive type of CMT (CMT4K), autosomal recessive demyelinating peripheral neuropathy (Echaniz-Laguna *et al.*, 2013). Moreover, copper dysfunction has also been reported in patients with *ATP7A* mutations associated with distal hereditary motor neuropathy similar to CMT. Interestingly patients with *ATP7A* mutations have decreased copper in some tissues, such as brain and liver and, in contrast, increased levels in other tissues including fibroblasts (Kaler, 2011).

Although more than 90 genes have been associated with CMT, a common mechanism remains elusive. The most common form of CMT2 is caused by mutations in the mitochondrial fusion factor *MFN2* (Zuchner *et al.*, 2004), and multiple CMT2 genes play a role in mitochondrial physiology. *SCO2* appears to be linked to copper metabolism, similar to *ATP7A*, which causes distal motor neuropathy. Copper is an essential metal and cofactor for many enzymes, such as the respiratory enzyme complex COX. Copper deficiency has been associated with a wide range of neurological diseases, including motor neuron disease (Weihl and Lopate, 2006). However, further studies will be required to elucidate the precise role of copper metabolism leading to motor neuropathy. In summary, this report provides the first description of CMT patients with *SCO2* mutations associated with decreased copper levels. This underlines the importance of copper homeostasis in the peripheral nervous system.

Acknowledgements

We would like to thank the patients and family members enrolled in this study.

Funding

The study was supported in part through the Inherited Neuropathy Consortium (U54NS065712), which is part of the Rare Disease Clinical Research Network (RDCRN), an initiative of the Office of Rare Diseases Research (ORDR), NCATS; The INC is funded through collaboration between NCATS and NINDS. The INC also receives support from the Muscular Dystrophy Association (MDA) and Charcot Marie Tooth Association (CMTA). The study was also supported by R01NS075764 (S.Z. and M.S. PIs) from NINDS, P01-HD08642 (E.A.S.) from NIH/NICHD, W-911F-15-1-0169 (E.A.S.) from the U.S. Department of Defense, and the Marriott Mitochondrial Disorders Clinical Research Network (E.A.S.).

Supplementary material

Supplementary material is available at *Brain* online.

References

Banci L, Bertini I, Ciofi-Baffoni S, Gerothanassis IP, Leontari I, Martinelli M, et al. A structural characterization of human SCO2. Structure 2007; 15: 1132–40.

Barrientos A, Barros MH, Valnot I, Rotig A, Rustin P, Tzagoloff A. Cytochrome oxidase in health and disease. Gene 2002; 286: 53–63.

Carson M. Ribbons 2.0. J Appl Crystallogr 1991; 24: 958–61.

Echaniz-Laguna A, Ghezzi D, Chassagne M, Mayencon M, Padet S, Melchionda L, et al. SURF1 deficiency causes demyelinating Charcot-Marie-Tooth disease. Neurology 2013; 81: 1523–30.

Gonzalez MA, Lebrigio RF, Van Booven D, Ulloa RH, Powell E, Speziani F, et al. GEnomes Management Application (GEM.app): a new software tool for large-scale collaborative genome analysis. Hum Mutat 2013; 34: 842–6.

Horng YC, Leary SC, Cobine PA, Young FB, George GN, Shoubridge EA, et al. Human Sco1 and Sco2 function as copper-binding proteins. J Biol Chem 2005; 280: 34113–22.

Kaler SG. ATP7A-related copper transport diseases-emerging concepts and future trends. Nat Rev Neurol 2011; 7: 15–29.

Kennerson ML, Nicholson GA, Kaler SG, Kowalski B, Mercer JF, Tang J, et al. Missense mutations in the copper transporter gene ATP7A cause X-linked distal hereditary motor neuropathy. Am J Hum Genet 2010; 86: 343–52.

Leary SC, Antonicka H, Sasarman F, Weraarpachai W, Cobine PA, Pan M, et al. Novel mutations in SCO1 as a cause of fatal infantile encephalopathy and lactic acidosis. Hum Mutat 2013; 34: 1366–70.

Leary SC, Cobine PA, Kaufman BA, Guercin GH, Mattman A, Palaty J, et al. The human cytochrome c oxidase assembly factors SCO1 and SCO2 have regulatory roles in the maintenance of cellular copper homeostasis. Cell Metab 2007; 5: 9–20.

Leary SC, Kaufman BA, Pellecchia G, Guercin GH, Mattman A, Jaksch M, et al. Human SCO1 and SCO2 have independent, cooperative functions in copper delivery to cytochrome c oxidase. Hum Mol Genet 2004; 13: 1839–48.

Marti-Renom MA, Stuart AC, Fiser A, Sanchez R, Melo F, Sali A, et al. Comparative protein structure modeling of genes and genomes. Annu Rev Biophys Biomol Struct 2000; 29: 291–325.

Papadopoulou LC, Sue CM, Davidson MM, Tanji K, Nishino I, Sadlock JE, et al. Fatal infantile cardioencephalomyopathy with COX deficiency and mutations in SCO2, a COX assembly gene. Nat Genet 1999; 23: 333–7.

Pronicki M, Kowalski P, Piekutowska-Abramczuk D, Taybert J, Karkucinska-Wieckowska A, Szymanska-Debinska T, et al. A homozygous mutation in the SCO2 gene causes a spinal muscular atrophy like presentation with stridor and respiratory insufficiency. Eur J Paediatr Neurol 2010; 14: 253–60.

Seburn KL, Morelli KH, Jordanova A, Burgess RW. Lack of neuropathy-related phenotypes in hint1 knockout mice. J Neuropathol Exp Neurol 2014; 73: 693–701.

Sievers F, Wilm A, Dineen D, Gibson TJ, Karplus K, Li W, et al. Fast, scalable generation of high-quality protein multiple sequence alignments using Clustal Omega. Mol Syst Biol 2011; 7: 539.

Soto IC, Fontanesi F, Liu J, Barrientos A. Biogenesis and assembly of eukaryotic cytochrome c oxidase catalytic core. Biochim Biophys Acta 2012; 1817: 883–97.

Stiburek L, Vesela K, Hansikova H, Pecina P, Tesarova M, Cerna L, et al. Tissue-specific cytochrome c oxidase assembly defects due to mutations in SCO2 and SURF1. Biochem J 2005; 392 (Pt 3): 625–32.

Strickland AV, Rebelo AP, Zhang F, Price J, Bolon B, Silva JP, et al. Characterization of the mitofusin 2 R94W mutation in a knock-in mouse model. J Peripher Nerv Syst 2014; 19: 152–64.

Telianidis J, Hung YH, Materia S, Fontaine SL. Role of the P-Type ATPases, ATP7A and ATP7B in brain copper homeostasis. Front Aging Neurosci 2013; 5: 44.

Valnot I, Osmond S, Gigarel N, Mehaye B, Amiel J, Cormier-Daire V, et al. Mutations of the SCO1 gene in mitochondrial cytochrome c oxidase deficiency with neonatal-onset hepatic failure and encephalopathy. Am J Hum Genet 2000; 67: 1104–9.

Weihl CC, Lopate G. Motor neuron disease associated with copper deficiency. Muscle Nerve 2006; 34: 789–93.

Williams JC, Sue C, Banting GS, Yang H, Glerum DM, Hendrickson WA, et al. Crystal structure of human SCO1: implications for redox signaling by a mitochondrial cytochrome c oxidase "assembly" protein. J Biol Chem 2005; 280: 15202–11.

Yang H, Brosel S, Acin-Perez R, Slavkovich V, Nishino I, Khan R, et al. Analysis of mouse models of cytochrome c oxidase deficiency owing to mutations in Sco2. Hum Mol Genet 2010; 19: 170–80.

Zuchner S, Mersiyanova IV, Muglia M, Bissar-Tadmouri N, Rochelle J, Dadali EL, et al. Mutations in the mitochondrial GTPase mitofusin 2 cause Charcot-Marie-Tooth neuropathy type 2A. Nat Genet 2004; 36: 449–51.